Rheol Acta
DOI 10.1007/s00397-010-0453-x

RAPID COMMUNICATION

The rheology of polymer solution elastic strands in extensional flow

Simon J. Haward · Jeffrey A. Odell · Zhuo Li · Xue-Feng Yuan

Received: 20 May 2009 / Revised: 25 March 2010 / Accepted: 2 April 2010

Abstract We apply micro-oscillatory cross-slot extensional flow to a semi-dilute poly(ethylene oxide) solution. Micro-particle image velocimetry (μPIV) is used to probe the real local flow field. Extreme flow perturbation is observed, where birefringent strands of extended polymer originate from the stagnation point. This coincides with a large increase in the extensional viscosity. The combination of stagnation point flow and μPIV enables us to investigate directly the stress and strain rates in the strand and so determine the true extensional viscosity of the localised strand alone. The Trouton ratio in the strand is found to be ∼4000, amongst the highest values of Trouton ratio ever reported. Consideration of the flow in the exit channels surrounding the highly elastic strand suggests a maximum limit for the pressure drop across the device and the apparent extensional viscosity. This has implications for the understanding of high Deborah number extensional thinning reported in other stagnation point flow situations.

Keywords Cross-slot · Extensional flow · Polymer solution · Rheology · Viscoelastic properties

S. J. Haward · J. A. Odell (✉)
HH Wills Physics Department, University of Bristol, Tyndall Avenue, Bristol BS8 1TL, UK
e-mail: jeff.odell@bristol.ac.uk

Z. Li · X.-F. Yuan
Manchester Interdisciplinary Biocentre and School of Chemical Engineering and Analytical Science, 131 Princess Street, Manchester M1 7DN, UK

Introduction

The study of extensional flows of polymer solutions is vital to improve the understanding of many complex natural and industrial processes involving both synthetic and biological polymeric fluids. Such processes include particle sedimentation, porous media flow (including enhanced oil recovery and filtration), inkjet printing, and numerous biological processes involving, e.g. mucins or synovial fluid.

It has been shown through studies of flow-induced birefringence, which indicates polymer orientation in flow, that stagnation point extensional flows of polymer solutions at sufficiently high strain rates can result in local regions of highly stretched polymer molecules (Keller et al. 1987; Odell et al. 1989). These regions form thin strands of localised stretching originating from the high strain associated with the stagnation point. These are more correctly sheets in 2D flows, but for simplicity, we will refer to all such structures as strands. Such stretching has also been demonstrated by direct measurement of end-to-end separation of fluorescently labelled DNA molecules (Perkins et al. 1997; Smith and Chu 1998). For dilute solutions, this conformational change is likely to result from a coil–stretch transition of the form predicted by De Gennes (1974) and for semi-dilute to concentrated solutions, a combination of molecular orientation and network deformation. Experimentally, these effects are found to coincide with large increases in flow resistance, probably most notably that observed in porous media flow of polymer solutions (Haas and Durst 1982; Delshad et al. 2008), which has often been linked to the increase in extensional viscosity when polymer molecules extend and align in flow.

Published online: 05 May 2010

For dilute solutions, the slender body theory for particles in Stokes flow can be used to estimate the increase in viscous drag when a polymer molecule undergoes a conformational change from fully coiled to fully stretched. This predicts that the ratio of the extensional to shear viscosity (the Trouton ratio) can be very high (Batchelor 1970; James and Sridhar 1995). In semi-dilute solutions and melt-flow, constitutive models such as Giesekus (1982), Oldroyd B, PTT (Phan-Thien and Tanner 1977), and Pom-Pom (McLeish and Larson 1998) have been applied with varying degrees of success. The Giesekus and Oldroyd B dumbbell model (which allows infinite extensibility) are unrealistic for strong extensional flow. The exponential PTT (EPTT) model is based upon the transient network approach and has enjoyed some success in modelling shear and extensional flows but often with many adjustable parameters, making modelling possible, but prediction impractical. Most constitutive models have great problems in dealing with the infinite residence time at the stagnation point (Dou and Phan-Thien 2001).

In practice, extremely high Trouton ratios have not been measured experimentally (James and Sridhar 1995; Odell and Carrington 2006; Gauri and Koelling 1997; Pipe and McKinley 2009); filament stretching rheometers typically measure values of order one tenth of that predicted by the slender body theory (Sridhar et al. 1991; McKinley et al. 2001). James and Sridhar attributed this chiefly to prohibition of full extension by intramolecular entanglements. In round-robin tests, values of the Trouton ratios of test fluids have varied by several orders of magnitude. It has been suggested that the key variable is the total strain to which the fluid is exposed (Sridhar 1990). This is exacerbated by the structural inhomogeneity of stranded structures, where the strand carries most or all of the extensional stress.

Modelling studies of idealised extensional flows, particularly those using finitely extensible nonlinear elastic dumbbells incorporating non-linear hydrodynamic friction, have shown that the viscosity increase due to extended polymers can cause considerable perturbations to the Newtonian flow field (Harlen et al. 1990, 1992; Remmelgas et al. 1999). Such effects have been reported previously in extensional flows in opposed jets (Lyazid et al. 1980) and cross-slots (Gardner et al. 1982). The prediction and observation of such large effects associated with polymer stretching in extensional flows and their widespread occurrence in important industrial and biological processes underlines the importance of improving understanding in this area. These early experimental works did not relate the flow perturbation to extensional viscosity, and particle imaging flow velocimetry has since improved to be a truly microscopic technique.

The purpose of this communication is to report investigations that concentrate upon the development of the inhomogeneous strand (or sheet) structures and probe the rheological properties of such strands and their effects on the whole flow field. The key to this is:

- Provision of well-defined and controlled micro flow fields to reduce inertial effects
- Optical analysis of molecular conformation in the strand
- Measurement of macroscopic shear and extensional viscosity
- μPIV to provide a quantitative analysis of the flow field and enable the assessment of local stress and strain rate.

Current and ongoing investigations in our laboratories are attempting to achieve this using the extensional flow oscillatory rheometer (EFOR) described by Odell and Carrington (2006). The EFOR is a new tool for the study of polymer solutions in stagnation point extensional flows, which can provide quantitative data on molecular strain, flow velocity and shear and extensional viscosities.

Experimental

The EFOR operates using two opposing pairs of piezo-actuated micro-pumps, with one pump on each limb of a cross-slot micro-channel. The first opposing pair of pumps run in phase with each other, with the second opposing pair running 180° out of phase with the first pair. The result is an oscillating planar extensional flow centred on the stagnation point at the centre of the cross (see Fig. 1). It should be noted that the periods of oscillation used are typically two orders of magnitude longer than the solution relaxation times, so that steady state is quickly achieved during each oscillation. The use of piezo-actuated micro-pumps facilitates exquisite control over pumped volume flow rates and therefore the strain rate applied to the polymer solution. The cross-slot we have used in this study was fabricated from stainless steel and has a width of $d = 200$ μm and a depth of $t = 1$ mm. This provides a 5:1 aspect ratio and so should be a reasonable approximation to a 2D flow.

The nominal extension rate, $\dot{\varepsilon}_{\mathrm{nom}}$, at volume flow rate Q, is given by:

$$\dot{\varepsilon}_{\mathrm{nom}} = \frac{2Q}{\mathrm{d}^2\mathrm{t}}. \tag{1}$$

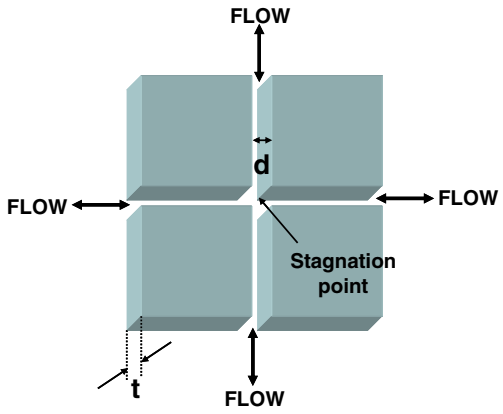

Fig. 1 Schematic diagram of the cross-slot flow cell of the EFOR, showing the principal dimensions and the location of the stagnation point

It should be noted that the true extensional rate in the strand, $\dot{\varepsilon}_{\text{true}}$ (determined, as we discuss later, directly from μPIV) is more important than the nominal value of the extension rate in study of the extensional flow. However, the nominal shear rate is a convenient quantity for setting up the experiments here.

Important flow relations are:

Nominal flow velocity:	Hydraulic diameter:
$U = \frac{Q}{\mathrm{d}t}$	$D_H = \frac{2\mathrm{d}t}{(\mathrm{d}+t)}$
Deborah number:	Reynolds number:
$De = \tau.\dot{\varepsilon}_{\text{true}}$	$Re = \frac{\rho U D_h}{\eta}$

where τ is the solution relaxation time, ρ the density and η the viscosity.

The pressure difference, ΔP, in the cross-slots is measured as a function of strain rate by a Druck differential pressure transducer connected across inlet and outlet channels. By disconnecting two of the pumps and simply measuring the pressure drop for flow of liquid around a corner of the cross-slot (ΔP_{shear}), we can measure the shear viscosity, η_{shear}, of the liquid. Assuming Poiseuille flow in a rectangular channel of total length 2L:

$$\eta_{\text{shear}} = \frac{\mathrm{d}^2 \Delta \mathrm{P}_{\text{shear}}}{24 U L} \tag{2}$$

Results for η_{shear} obtained with Eq. 2 agree well with results from a conventional ARES Couette rotational rheometer.

By measuring the pressure drop with all four pumps running (ΔP_{total}), we can find the excess pressure drop due the extensional part of the flow field. Assuming the extensional viscosity in the birefringent strand, $\eta_{\text{ext}} >> \eta_{\text{shear}}$, and therefore dominates the excess pressure drop, we can obtain a measure of the extensional viscosity of the strand using:

$$\eta_{\text{ext}} = \frac{\Delta \mathrm{P}_{\text{total}} - \Delta \mathrm{P}_{\text{shear}}}{\dot{\varepsilon}_{\text{true}}} \cdot \frac{\mathrm{d}}{\mathrm{w}} \tag{3}$$

where w is the width of the birefringent strand (full width at half maximum intensity) and $\dot{\varepsilon}_{\text{true}}$ is the actual extensional rate in the strand.

In terms of the stress in the strand

$$\eta_{\text{ext}} = \frac{T_s}{\dot{\varepsilon}_{\text{true}}} \tag{4}$$

we propose to determine η_{ext} directly *in the strand* by using μPIV to assess the real extensional rate, $\dot{\varepsilon}_{\text{true}}$, and stress, T_{s}.

Observing the stagnation point through polarisers crossed at ±45° to the direction of flow allows detection and measurement of flow-induced birefringence. Birefringence can be compared with models to give an indication of accumulated polymer molecular strain. To provide information on the interaction between the flow field and polymer conformation, the EFOR has been designed to integrate with a TSI μPIV system, enabling quantitative assessment of flow-field perturbation due to the stretching polymer on length scales down to 3 μm.

Our test fluid was an aqueous solution of poly(ethylene oxide) (PEO) provided by Dow Chemicals. The weight average molecular mass is 4.82 M (g/mol), and the polydispersity index, $M_{\text{w}}/M_{\text{n}}$, is 7.5. The mean radius of gyration (R_{g}) of PEO molecules in water can be estimated by:

$$\langle R_{\text{g}} \rangle = 0.0215 M_{\text{w}}^{0.583} \text{nm} \tag{5}$$

(Devenand and Selser 1991). Based on this light scattering data and assuming simple cubic packing of polymer coils in the solution, we estimate the overlap concentration c^* to be ~0.02 wt% (Graessley 1980). Our test solution was $c = 0.3$ wt%, indicating that it is in the semi-dilute regime with c/c^* approximately 15.

The zero shear viscosity was measured at $\eta_0 \sim 10$ mPa.s and the relaxation time at $\tau \sim 5 \times 10^{-3}$ s using an ARES rheometer and a CaBER extensional rheometer, respectively. For μPIV measurements, the solution was seeded with 1-μm diameter fluorescent particles at a concentration of 0.008 wt%.

The flow in the cross-slot was driven by applying oscillating triangular voltage profiles (corrected for hysteresis) to the piezo micro-pumps. This resulted in a constant nominal shear rate (dependent on voltage am-

plitude and frequency) for half a cycle period (generally 1 s), before reversal of the flow. The rise time for the pressure drop to steady state after each flow reversal was 100–150 ms, which provided an 850–900-ms window of steady-state flow before the subsequent flow reversal. All pressure, birefringence and μPIV measurements were taken during this steady-state window.

A recent paper (Haward et al. 2010) investigates the behaviour of dilute well-defined monodisperse solutions of a-PS, in terms of strand properties and flow modification.

Results and discussion

For our 0.3-wt% semi-dilute solution, Fig. 2a shows a typical birefringent strand observed along the centre line of the out-flowing channels of the cross-slots at $\dot{\varepsilon}_{\mathrm{nom}} = 1{,}800\,\mathrm{s}^{-1}$. The strand is long and closely localised along streamlines that pass close to the stagnation point at the centre of the cross. The strand fades towards the outlet entrances purely because this is at the extreme edge of the illuminated observation area at the centre of the cross-slot. In fact the birefringence persists along the entire length of the outlet channel, which is 1.2 mm long. This strain rate represents approximately the limit of linear behaviour and, as we shall see, the maximum of extensional viscosity and will be taken as our reference point for subsequent analysis.

Figure 2b–d show how the birefringence develops at higher nominal extension rates, with a broadened strand at 3,600 s^{-1}, a "pipe" structure at 7,200 s^{-1} and broad generalised birefringence at 14,400 s^{-1}. This behaviour is very similar to that reported by Keller et al. (1987).

Figure 3a shows an instantaneous vector map of the steady-state velocity field in the locality of the cross obtained under the same conditions as Fig. 2a. This is a 2D 13.6-μ thick slice through the mid-plane of the cross-slot. In our experiments with PEO solutions, we saw no evidence of the elastic instabilities and asymmetric flow observed by Arratia et al. (2006) with an ultrahigh molecular weight polyacrylamide solution and simulated by Poole et al. (2007), even though our experiments extend to higher *De*.

Analysis of the velocimetry data from Fig. 3a provides the velocity profiles shown in Fig. 3b–d. Figure 3b shows typical Poiseuille-like velocity profiles across an inlet channel. In contrast, Fig. 3c shows a radically different flow velocity profile across an exit channel as the flow leaves the stagnation point. In this

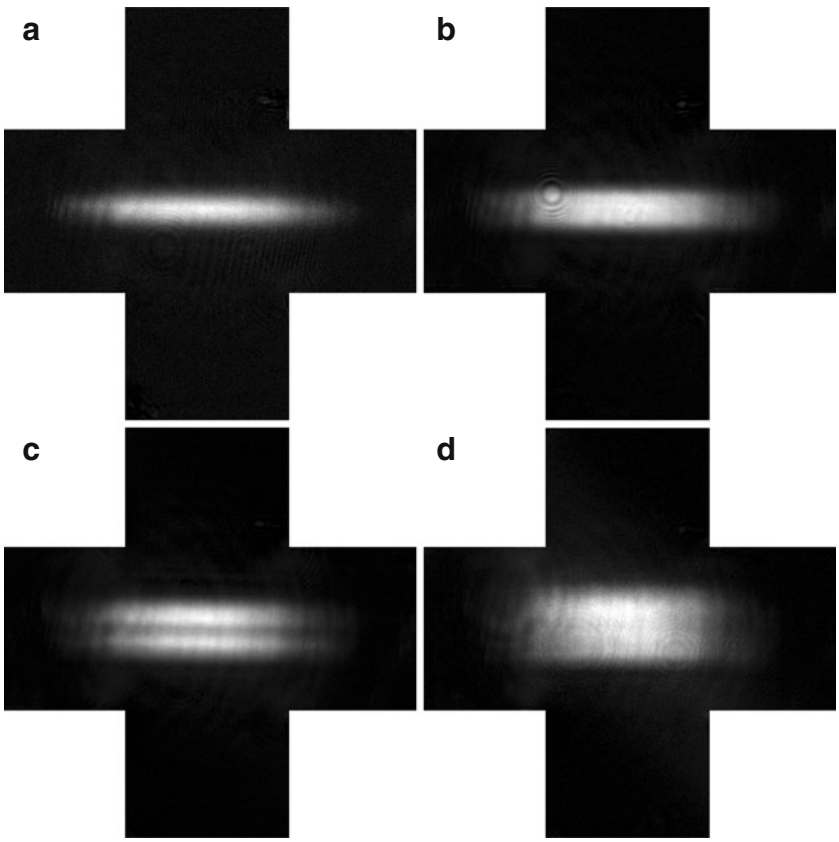

Fig. 2 Typical examples of birefringent strand structures observed in the cross-slots for flow of 0.3 wt% 4.82-M PEO at the following nominal shear rates: **a** 1,800 s^{-1}, **b** 3,600 s^{-1}, **c** 7,200 s^{-1} and **d** 14,400 s^{-1}. The exit channel is horizontal. The intensity scale is non-linear

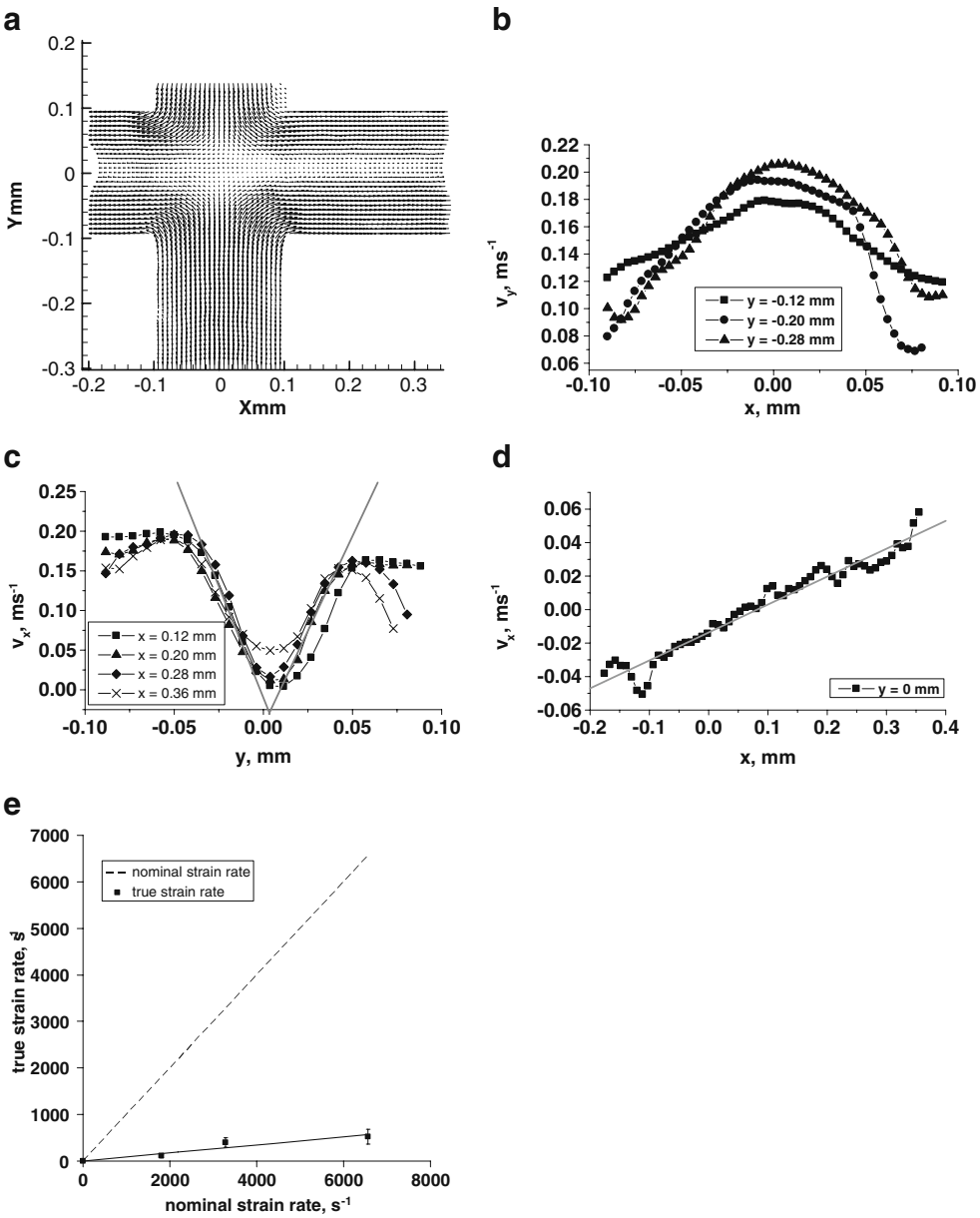

Fig. 3 **a** Vector map of flow field in the cross-slots for 0.3 wt% 4.82-M PEO at a nominal strain rate of 1,800 s^{-1} (the outlet channel is horizontal), **b** velocity profiles across an inlet channel, **c** velocity profiles across an outlet channel, **d** velocity profile along the symmetry axis of the outlet channel. **e** True strain rate in the birefringent strand as a function of the nominal shear rate

study, on the central axis of the channel, close to the stagnation point, the flow velocity is effectively reduced to zero and only increases slowly with distance along the channel. The highest flow velocities are recorded in the narrow regions between the stretched strand and the walls of the channel. Finally, Fig. 3d shows the flow velocity along the entire length of the central axis of the outlet channels, going through the stagnation point at $x = 0$.

Figure 3c–d allows us to make some interesting calculations. Most obviously the gradient of Fig. 3d (indicated by the solid grey line) provides the actual value of the extensional rate within the birefringent strand. This gives an extensional rate of $\dot{\varepsilon}_{\text{true}} = (110 \pm 5)\,\text{s}^{-1}$, roughly one sixteenth of $\dot{\varepsilon}_{\text{nom}} = 1{,}800\,\text{s}^{-1}$ based on Eq. 1. The value $\dot{\varepsilon}_{\text{true}} = 110\,\text{s}^{-1}$ is lower than the reciprocal of the relaxation time measured using the CaBER extensional rheometer, giving a Deborah number of ~0.5 and clearly indicating the strong resistance of the polymer solution to stretch.

The data of Fig. 3c can be used to estimate directly the stress T_s applied to the birefringent strand by the fluid flowing between the strand and the walls of the outlet channel. It is this stress that is maintaining the strain in the strand. The strand is essentially an elastic sheet, provided that the local extensional strain rate within the sheet exceeds the reciprocal of its relaxation time. This sheet is capable of extremely high elastic

forces to support the integrated shear stresses in the exit channel. Looking at the gradient of the steep parts of the curves in Fig. 3c (indicated by the solid grey lines), we can estimate the shear rate of the fluid near the strand to be ~4,000 s^{-1} on each side of the strand. Given a shear viscosity of 0.01 Pa.s, this provides a total stress of ~80 Pa. The strand extends for 1.2 mm downstream and is 1 mm deep (the depth of the flow cell); we therefore have a total force on the strand of ~96 μN. Estimating the width of the strand from Fig. 2a to be ~0.02 mm gives a tension in the strand of 4,800 Pa. Division by $\dot{\varepsilon}_{true} = 110\,s^{-1}$ gives an estimate of the extensional viscosity of ~43.6 Pa.s and a Trouton ratio of ~4,360. Due to the low values of solution viscosity, it did not prove possible to obtain reliable extensional viscosity and Trouton ratio data from the CaBER experiments.

Figure 4a shows the shear and extensional viscosity of the polymer solution, calculated from the measured pressure drops using Eqs. 2 and 3, as a function of the true extensional rate in the cross-slots. The shear viscosity is well behaved and displays a near constant viscosity of ~0.01 Pa.s with slight shear thinning across the strain rate range, close to the values measured using the ARES. It should be noted that the ARES experiments were conducted using a constant strain rate Couette geometry, which is not directly comparable with the Poiseuille-type channel flow of the EFOR.

The extensional viscosity shows a markedly different behaviour, with a rapid increase to ~27 Pa.s at $\dot{\varepsilon}_{true} \sim 60\,s^{-1}$, before a gradual reduction to ~9 Pa.s. The highest Trouton ratio that we measure by this method is therefore Tr = 27/0.01 = 2,700. The final value of Trouton ratio for higher strain rates is Tr = 9/0.01 = 900. The reduction in extensional viscosity beyond $\dot{\varepsilon}_{true} = 60\,s^{-1}$ is probably not explained by inertial effects since the Reynolds number is only ~1 at this point. It is also not due to mechanical degradation of the polymer because each data point on Fig. 4a was collected with fresh polymer solution in the cross-slot. In addition, as can be seen in Fig. 4b, the measured birefringence continues to increase smoothly between $\dot{\varepsilon}_{true} = 60\,s^{-1}$ and 1,500 s^{-1}, further discounting inertia and degradation as possible causes.

We believe the apparent reduction in extensional viscosity is explained by flow perturbation. As the strain rate increases, the strand broadens. In the limit of high Trouton ratio, we can regard the strand as being elastic and inextensible compared to the surrounding fluid, which has an almost constant shear viscosity. The effect of this is to have regions in the channel surrounding the strand of higher, but limited, shear rate. This leads to an effective maximum pressure drop limited by the shear

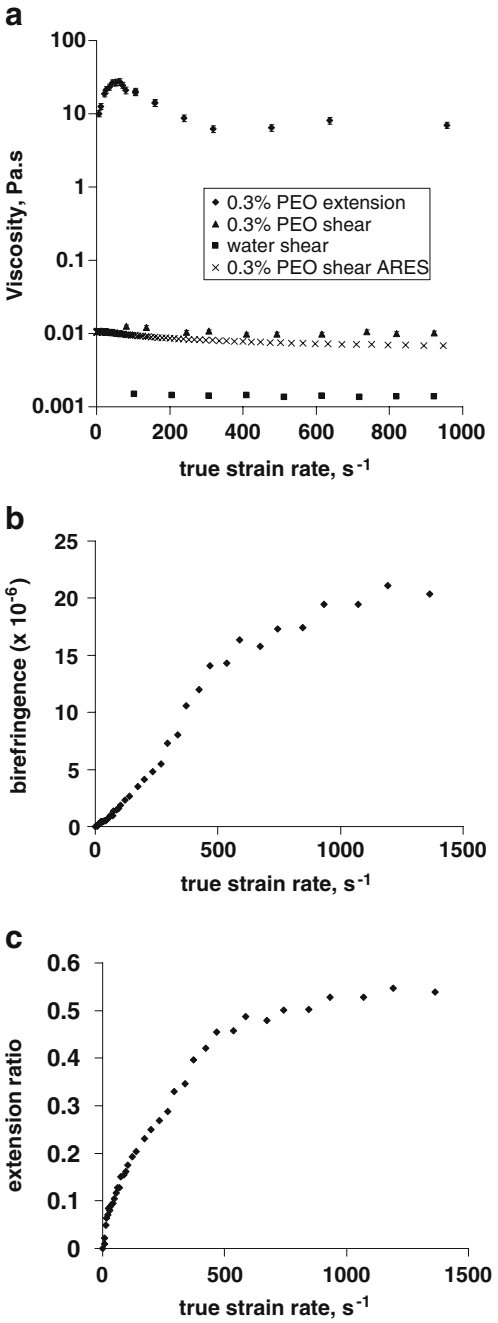

Fig. 4 **a** Viscosity (determined from EFOR pressure drop measurements and ARES Couette), **b** stagnation point birefringence and **c** fractional molecular strain as a function of the true strain rate in the birefringent strand, 0.3 wt% 4.82-M PEO

viscosity, explaining the apparent drop in extensional viscosity determined from the pressure drop. This may be generalised to other strand developing flow geometries such as porous media flows and flows around spheres, where flow resistance is calculated by pressure drops divided by nominal strain rate or superficial flow velocity. A plateau or drop in derived flow resistance is a commonly observed phenomenon and has previ-

ously been explained by inertial effects, polymer entanglements and polymer degradation (Odell et al. 1989; Haas and Durst 1982; Odell and Carrington 2006). It should be noted that the EPTT model can reproduce the drops in extensional viscosity (Sun et al. 2000).

The birefringence in Fig. 4b shows a progressive increase from a true strain rate as low as $\dot{\varepsilon}_{\text{true}} \sim 20\ \text{s}^{-1}$. This is ten times lower than the reciprocal of the relaxation time of 5 ms measured using the CaBER extensional rheometer. We attribute this to the known presence of a very high molecular weight tail, which has a much longer than average relaxation time. The birefringence rises to a maximum value of $\Delta n \sim 2.2 \times 10^{-5}$ at $\dot{\varepsilon}_{\text{true}} = 1{,}300\ \text{s}^{-1}$, then plateaus. The birefringence can be used to obtain an estimate of molecular strain (extension ratio) using the approximation to the inverse Langevin function of Treloar (1975) and an estimate for the birefringence of a solution of fully stretched PEO molecules. This is taken to be $\Delta n_0 = 0.035c$, obtained from measurements with ultra-stretched PEO fibres (Kim and Porter 1985). The calculated extension ratio is shown in Fig. 4c. The value of the extension ratio rises progressively to a plateau of 0.55. At our reference strain rate ($\dot{\varepsilon}_{\text{nom}} = 1{,}800\ \text{s}^{-1}$, $\dot{\varepsilon}_{\text{true}} = 110\ \text{s}^{-1}$), we estimate an extension ratio of ~0.22 indicating that molecules are stretched to roughly one fifth of their contour length. For a 4.82-M PEO, this is equivalent to a molecular strain of ~12.

Following James and Sridhar (1995), according to Batchelor's theory, if the polymer sample was monodisperse $M_{\text{w}} = 4.82 \times 10^6$ and all molecules were fully stretched to their contour length, L, the Trouton ratio would be ~400,000 (Batchelor 1970). Since Batchelor's formula depends on L^3 and is only weakly dependent on the molecular diameter, we might estimate a theoretical Trouton ratio for our birefringent strand at $\dot{\varepsilon}_{\text{nom}} = 1{,}800\ \text{s}^{-1}$ (in which molecules stretched to one fifth of their contour length) of $\text{Tr} \sim 3{,}200$. This is in reasonable accord with both our experimental peak value of 2,700 from Eq. 3 and our estimate of 4,360 from PIV measurements and Eq. 4. More correctly, semi-dilute or network models should be applied to allow for the entangled solutions. It is expected that the Trouton ratio would be lowered in such models as EPTT.

Conclusions

In summary, we have presented preliminary experimental results from an oscillatory cross-slot flow experiment in which we can measure pressure, birefringence and flow field. We have demonstrated that even for modest applied strain rates and relatively low values of polymer strain, semi-dilute PEO solutions exhibit remarkable extension thickening properties providing extraordinarily high Trouton ratios of up to 4,000. We have shown that where the polymer molecules extend flowing away from the stagnation point, there is a dramatic perturbation of the flow field, which severely limits the actual value of the strain rate applied to the polymer. This results in an actual strain rate 12 times lower than would be expected based on the flow geometry and volume flow rate (as per Eq. 1). Our results clearly demonstrate the dominance of the extensional component in the flow field due to the stagnation point and that this dominates the resulting behaviour of the polymer in flow. This must be considered of great importance in all real flows with extensional components such as porous media flow, inkjet printing, sedimentation and many biologically relevant processes.

Acknowledgement We gratefully acknowledge the financial support of the Engineering and Physical Sciences Research Council of the UK.

References

Arratia PE, Thomas CC, Diorio J, Gollub JP (2006) Elastic instabilities of polymer solutions in cross channel flow. Phys Rev Lett 96:144502

Batchelor GK (1970) Slender-body theory for particles of arbitrary cross-section in Stokes flow. J Fluid Mech 44:419–440

De Gennes PG (1974) Coil–stretch transition of dilute flexible polymers under ultrahigh velocity gradients. J Chem Phys 60:5030–5042

Delshad M, Kim DH, Magbagbeola O, Huh C, Pope G, Tarahhom F (2008) Mechanistic interpretation and utilization of viscoelastic behavior of polymer solutions for improved polymer-flood efficiency. SPE/DOE Symposium on Improved Oil Recovery, 20–23 April 2008, Tulsa, Oklahoma, USA

Devenand K, Selser JC (1991) Asymptotic behaviour and long-range interactions in aqueous solutions of poly(ethylene oxide). Macromolecules 24:5943–5947

Dou H, Phan-Thien N (2001) Numerical difficulties at high elasticity for viscoelastic flow past a confined cylinder. Int J Comput Eng Sci 2(2):249–266

Gardner K, Pike ER, Miles MJ, Keller A, Tanaka K (1982) Photon-correlation velocimetry of polystyrene solutions in extensional flow fields. Polymer 23:1435–1442

Gauri V, Koelling KW (1997) Extensional rheology of concentrated poly(ethylene oxide) solutions. Rheol Acta 36:555–567

Giesekus H (1982) A simple constitutive equation for polymer fluids. J Non-Newton Fluid Mech 11:69–09

Graessley WW (1980) Polymer chain dimensions and the dependence of viscoelastic properties on concentration, molecular weight and solvent power. Polymer 21:258–262

Haas R, Durst F (1982) Viscoelastic flow of dilute polymer solutions in regularly packed beds. Rheol Acta 21:566–571

Harlen OG, Rallison JM, Chilcott MD (1990) High-Deborah-number flows of dilute polymer solutions. J Non-Newton Fluid Mech 34:319–349

Harlen OG, Hinch EJ, Rallison JM (1992) Birefringent pipes: the steady flow of a dilute polymer solution near a stagnation point. J Non-Newton Fluid Mech 44:229–265

Haward S, Odell JA, Li Z, Yuan X-F (2010) Extensional rheology of dilute polymer solutions in oscillatory cross-slot flow: the transient behaviour of birefringent strands. Rheol Acta. doi:10.1007/s00397-009-0420-6

James DF, Sridhar T (1995) Molecular conformation during steady-state measurements of extensional viscosity. J Rheol 39:713–724

Keller A, Müller AJ, Odell JA (1987) Entanglements in semi-dilute solutions as revealed by elongational flow studies. Prog Colloid & Polym Sci 75:179–200

Kim BS, Porter RS (1985) Uniaxial draw of poly(ethylene oxide) by solid state extrusion. Macromolecules 18:1214–1217

Lyazid A, Scrivener O, Teitgen R (1980) In: Astarita G, Marrucci G, Nicolais L (eds) Rheology, vol 2. Plenum, New York, pp 41–148

McKinley GH, Brauner O, Yao M (2001) Kinematics of filament stretching in dilute and concentrated polymer solutions. Korea-Australia Rheology J 13:29–35

McLeish TCB, Larson RG (1998) Molecular constitutive equations for a class of branched polymers: the pom-pom polymer. J Rheol 42:81–110

Odell JA, Carrington SP (2006) Extensional flow oscillatory rheometry. J Non-Newton Fluid Mech 137:110–120

Odell JA, Keller A, Müller AJ (1989) Extensional flow behaviour of macromolecules in solution. In: Glass JE (ed) Polymers in aqueous media. American Chemical Society, Washington, pp 193–244

Perkins TT, Smith DE, Chu S (1997) Single polymer dynamics in an elongational flow. Science 276:2016–2021

Phan-Thien N, Tanner RI (1977) A new constitutive equation derived from network theory. J Non-Newton Fluid Mech 2:353–365

Pipe J, McKinley GH (2009) Microfluidic rheometry. Mech Res Commun 36:110–120

Poole RJ, Alves MA, Oliveira PJ (2007) Purely elastic flow asymmetries. Phys Rev Lett 99:164503

Remmelgas J, Singh P, Leal LG (1999) Computational studies of nonlinear elastic dumbbell models of Boger fluids in a cross-slot flow. J Non-Newton Fluid Mech 88:31–61

Smith DE, Chu S (1998) Response of flexible polymers to sudden elongational flow. Science 281:1335–1340

Sridhar T (1990) An overview of the project M1. J Non-Newton Fluid Mech 35:85–92

Sridhar T, Tirtaatmadja V, Nguyen DA, Gupta RK (1991) Measurement of extensional viscosity of polymer solutions. J Non-Newton Fluid Mech 40:271–280

Sun N, Chan Man Fong CF, De Kee D (2000) A non-affine transient network model. Rheol Acta 39:174-179

Treloar LKG (1975) The physics of rubber elasticity, 3rd edn. Clarendon Press, Oxford